Physica Medica 57 (2019) 17–24

Contents lists available at ScienceDirect

Physica Medica

journal homepage: www.elsevier.com/locate/ejmp

Original paper

Calculating organ and effective doses in paediatric interventional cardiac radiology based on DICOM structured reports – Is detailed examination data critical to dose estimates?

Angeliki Karambatsakidou[a,b,*], Artur Omar[a,b], Annette Fransson[a,b], Gavin Poludniowski[a,b]

[a] Department of Medical Radiation Physics and Nuclear Medicine, Karolinska University Hospital, 171 76 Stockholm, Sweden
[b] Department of Oncology-Pathology, Karolinska Institutet, 171 76 Stockholm, Sweden

ARTICLE INFO

Keywords:
Paediatric interventional cardiology
Organ doses
Conversion coefficients
RDSR

ABSTRACT

Purpose: To estimate effective dose (E), equivalent organ doses (H_T) and associated conversion coefficients ($CC_{E:KAP}$ = E/KAP, $CC_{HT:KAP}$ = H_T/KAP; KAP = Kerma-area product) in paediatric cardiac interventions, using detailed exposure data from radiation dose structured reports (RDSR). These "RDSR dose estimations" have been compared with estimations performed using the approach currently implemented in the clinic that is based on a simplified assumptions method (SAM).

Methods: The Monte Carlo system PCXMC, incorporated into a previously developed framework, was used to calculate E and H_T for 202 children. The calculations were performed with input values from RDSR, and also using simplified assumptions, including fixed nominal values for the focus-skin distance, collimated beam size, irradiation geometry and patient size (age, weight and height).

Results: Mean H_T to critical organs were: 5–25 mSv (lungs), 5–8 mSv (breasts) and 5–22 mSv (heart), with the lower and upper end of the doses associated with the neonatal and 15 years group, respectively. The associated mean $CC_{HT:KAP}$ for the different age groups were: 9.4–1.6 mSv/Gycm^2 (lungs), 8.9–0.54 mSv/Gycm^2 (breasts) and 9.3–1.4 mSv/Gycm^2 (heart).

Conclusions: The extension of the concept of a conversion coefficient for H_T is introduced and $CC_{HT:KAP}$ values for paediatric cardiac interventions divided in age groups are presented. This method of linking the KAP to H_T is intended for use in epidemiological/cohort studies or in clinics that do not have access to RDSR. Further, the population-averaged conversion coefficients for the critical organs estimated from RDSR, displayed no statistically significant difference compared with the SAM approach.

1. Introduction

Interventional radiological procedures can result in high patient doses. This is of special concern in case of children as they are more radiosensitive than adults and with a correspondingly increased risk for cancer induction [1–4]. Children undergoing cardiac radiological interventions can receive high doses [5,6] related either to the need for repeated procedures, to the complexity of the intervention, or to both. Although the exposure of patients to x rays during image-guided interventional procedures is of concern, the use of minimally invasive techniques is preferred over invasive open-heart surgery due to the increased risk of medical complications [7]. As such, the use of minimally invasive x-ray interventional procedures is on a steady rise [8], which implies a need to better understand the effective doses and especially the organ doses delivered to paediatric patients undergoing cardiac catheterizations. Moreover, the lack of conversion coefficients for equivalent organ doses have been raised in the review paper by Hill et al. [9]. Such conversion coefficients could be an important tool for future, much needed, epidemiologic studies on the effects of low-dose ionization radiation [10].

The radiation dose indicator reported by catheterization x-ray equipment, kerma-area product (KAP), provides only information about the total amount of radiation used during the procedure and thus does not account for the age-dependent variation in radiation sensitivity. This implies that the KAP-value must be linked to effective dose (E) or preferably to equivalent organ dose (H_T) to be able to give an estimate on the radiation effects.

Several studies have estimated H_T and E in paediatric interventional cardiology [11–14], but several notable simplifications have typically been used to determine H_T and E from interventional procedures in

* Corresponding author at: Department of Medical Radiation Physics and Nuclear Medicine, Karolinska University Hospital, 171 76 Stockholm, Sweden.
E-mail address: angeliki.karambatsakidou@sll.se (A. Karambatsakidou).

https://doi.org/10.1016/j.ejmp.2018.12.008
Received 22 May 2018; Received in revised form 9 November 2018; Accepted 12 December 2018
Available online 19 December 2018

order to describe the irradiation events. Modern angiography equipment produces DICOM Radiation Dose Structured Reports (RDSR) [15], which together with Monte Carlo calculations of energy deposition, can be used to estimate H_T and E more accurately.

The aim of this work was to calculate H_T and E and associated conversion coefficients in children with congenital heart disease undergoing interventional cardiac radiological procedures. Two methods for estimating the radiation dose have been compared: (i) based on detailed information about the exposure geometry and settings, extracted from RDSR, (ii) based on the information from the patient radiation dose sheet obtained from the x-ray system at the end of each procedure, where some typical assumptions about the exposure geometry and settings have to be made as this information is missing (referred to as simplified assumptions method; SAM). Further, conversion coefficients for different ages are presented for convenient conversion of the readily measurable quantity kerma-area product (KAP) to patient dose. This is intended for use in clinics that do not have the full RDSR-based framework [16] and for retrospective analyses with large paediatric cohorts. Notably, in this study, the $CC_{HT:KAP}$ is presented for the first time in paediatric cardiac catheterization procedures.

2. Materials and methods

2.1. X-ray equipment

All procedures were carried out on a biplane Philips AlluraClarity x-ray system (Philips, Best, The Netherlands) with integrated KAP-meters (Diamentor; PTW-Freiburg, Germany) fitted on each x-ray tube housing. The accuracy of the integrated KAP-meters was checked against a reference KAP meter (Doseguard 100 (VacuTec 70157); RTI Electronics AB, Mölndal, Sweden) calibrated at the Swedish secondary standard dosimetry laboratory. A tandem calibration method by Toroi et al. [17] was used. The imbedded KAP-meter was checked for beam qualities RQR6 (80 kVp; 3.0 mm Al total filtration) and RQA6 (80 kVp; 29 mm Al total filtration), resulting in $< 10\%$ in deviation. The x-ray system has two (biplane) flat panel detectors (FD) with three magnification modes (diagonal image receptor size of: 15, 20 and 25 cm) which were equipped with antiscatter grids (ratio, 13:1). The air kerma rate settings at the detector surface (without grid) were 0.08 μGy per frame, 0.06 μGy per frame and 0.05 μGy per frame in fluorography mode, and 0.18, 0.14 and 0.10 μGy/s in fluoroscopy mode. The system uses automatic dose rate control to automatically selects beam quality parameters based on the type of examination and patient size [18]. The inherent filtration of the tube was 3.5 mm aluminium (Al) equivalence and the additional filtration was 1.0 mm Al + 0.4 mm copper (Cu) in both fluorography and fluoroscopy mode (all modes). The cardiological procedures were performed with an image acquisition rate of 15 or 25 frames/s.

2.2. Patient cohort

The cohort included 202 paediatric patients (108 female, 94 male) ranging from new-borns to 18 years old. The patients were divided into age intervals around the applicable phantom sizes in the PCXMC software (0, 1, 5, 10 and 15 years) [19] and consisted of 40 in the age group 0 years [0–0.5) years, 54 in the age group of 1 year [0.5–2.5) years, 65 in the age group of 5 years [2.5–7.5) years, 27 in the age group of 10 years [7.5–12.5) years and 16 in the age group of 15 years [12.5–18.0) years. All patients suffered from congenital heart disease and underwent cardiac catheterizations between 2013 and 2016. The diagnostic procedures included evaluations of anatomy and/or hemodynamics in complex congenital cardiac malformations. The interventional procedures included balloon pulmonary valvuloplasty, balloon angioplasty and/or stent treatment for obstructive lesions, transcatheter vascular occlusions, transcatheter device closure of atrial septal defects and transcatheter pulmonary valve replacement. Heart muscle biopsies, post transplantation, were also performed. The study was approved by the regional ethical review board in Stockholm, with the authorization no 2016/2400-31, 11 January 2017.

2.3. Equivalent organ dose and effective dose

Effective dose is defined for a reference adult person and has been used as an “indicator” of risk for late effects of radiation. It is now being replaced by the equivalent dose (H_T) [20]. The role of E in comparing risks from different types of radiological procedures or the same procedure performed in different centers, is, however, still of interest, provided attention is paid to the fact that it cannot be used to indicate absolute risk even in an adult individual and ought to be interpreted with even more caution for a paediatric population [21]. We suggest that estimates of E reported in the current work could be used for such inter-procedural comparisons.

The equivalent organ dose and the effective dose (ICRP Publication 103 [20]) were determined using a previously developed framework for systematic patient organ dose estimation in interventional radiology based on input data from DICOM RDSR (for the RDSR approach) or from patient radiation dose sheets (for the SAM approach). The method has been described in detail in Ref. [16]. However, for completeness, it is briefly summarised as follows. First, the incident air kerma is determined (considering the transmission through the patient table), based on RDSR data that characterises the x-ray beam (e.g., tube kilovoltage) and the exposure geometry (e.g., collimated beam size). The geometrical relation between the projected x-ray beam and the patient's anatomy is then reconstructed using RDSR data (referred to as the target-centric approach in Ref. [16]). Lastly, the calculated air kerma is converted into equivalent organ dose by Monte Carlo dose calculations.

The Monte Carlo system PCXMC [19] was used to determine the equivalent organ dose by simulating the transport of photons in a computational phantom. The paediatric models in PCXMC were created from the slightly modified and updated computational phantoms (0, 1, 5, 10 and 15 years) of Cristy et al. [21]. The organ dose calculations were performed automatically using a script that (i) generates an input file for each separate irradiation event included in an RDSR file, (ii) initiates PCXMC by command line, and (iii) extracts data from the generated output file.

Two sets of calculations were performed to assess the impact of using simplified assumptions about the exposure settings and geometry in the absence of more accurate RDSR information; the settings used for the two sets of calculations are summarised in Table 1, where SAM refers to the simplified assumptions method based on information available from the patient radiation dose sheet obtained from the x-ray system at the end of each procedure, and RDSR refers to the more accurate method based on RDSR data. The following typical assumptions [11–14,22,23] have been considered:

- **SAM**: A fixed collimated beam size that depends on the patient age was assumed (neonate, $7 \times 7\,cm^2$; 1 year, $8 \times 8\,cm^2$; 5 years, $9.5 \times 9.5\,cm^2$; 10 years, $11 \times 11\,cm^2$; 15 years, $12 \times 12\,cm^2$). **RDSR**: The collimated beam size reported in the RDSR for each separate irradiation event (exposure series) was used.
- **SAM**: The x-ray beam was assumed to be centred on the heart for the entirety of the procedure. **RDSR**: The imaging of body regions other than the heart (e.g., imaging during catheter insertion) were accounted for based on information included in the RDSR about the position of the x-ray beam and the patient table.
- **SAM**: A fixed focus-to-skin distance (FSD) of 60 cm was assumed. **RDSR**: Although information about the FSD is not included in the RDSR, it was inferred from the parameters that describe the exposure geometry (as described in Ref. [16]): the length of a ray line traced from the x-ray source to the surface of a computational phantom that mimics the patient habitus was used for the FSD.
- **SAM**: The KAP contribution of the fluoroscopy imaging was

Table 1
Input parameters for the Monte Carlo system PCXMC. The parameters correspond to those used for the RDSR methodology and the simplified assumptions used in the clinic today (SAM).

Method	KAP	Collimated beam size	Beam position	FSD	Fluoroscopy	Tube potential[1]	Total filtration	Projection angle[2]	Oblique angle[3]	Patient size
RDSR	RDSR	RDSR	RDSR	RDSR	RDSR	RDSR	RDSR	RDSR	RDSR	HIS
SAM	Dose sheet[4]	Fixed[5]	Heart[6]	Fixed[7]	Averaged[8]	Dose sheet [4]	Dose sheet [4]	Dose sheet [4]	Dose sheet [4]	PCXMC[9]

KAP, kerma-area product; FSD, focus-skin distance; RDSR, radiation dose structured report; SAM, simplified assumptions method.
[1] Tube potential from fluorography.
[2] Detector rotation angle from right anterior oblique (RAO) to left anterior oblique (LAO) with origin perpendicular to patient's chest.
[3] Detector rotation angle from caudal (CAU) to cranial (CRA) with origin perpendicular to patient's chest.
[4] The parameters from the patient radiation dose sheet obtained at the end of each procedure from the x-ray system.
[5] The beam size (collimated beam width and height) is fixed for each age group (neonate, $7 \times 7\,cm^2$; 1 year, $8 \times 8\,cm^2$; 5 years, $9.5 \times 9.5\,cm^2$; 10 years, $11 \times 11\,cm^2$; 15 years, $12 \times 12\,cm^2$; Ref [20]).
[6] The irradiation field was centered on the heart throughout the procedure.
[7] The focus-to-skin distance (FSD) is 60 cm for all beam angulations and for all patients.
[8] The KAP contribution of the fluoroscopy imaging was proportionally distributed among the fluorography imaging.
[9] The patient size (weight, height) is the same within each age group as defined in PCXMC.

proportionally distributed among the fluorography imaging (referred to as stationary image acquisition in the DICOM standard) **RDSR**: The settings reported in the RDSR for each separate fluoroscopy event were used. This includes settings such as tube kilovoltage, spectral filtration, exposure geometry, etc.

- **SAM**: The nominal size (weight, height) of the phantom models included in the PCXMC Monte Carlo system were used, i.e., one of five fixed patient sizes (weight, height) was selected, depending on age. **RDSR**: The size of each phantom model was scaled to match the height and weight of each patient. Although this kind of patient information is included in the RDSR for some x-ray systems, in this study it was extracted from the Hospital Information System (HIS).

2.4. Dose conversion coefficient

Conversion coefficients for effective dose ($CC_{E:KAP}$) were determined from the ratio E/KAP. The average value for an age category was determined as the mean of the values for the individuals. The use of a single $CC_{E:KAP}$ for each age group was considered plausible because the dependence of the irradiation geometry on E is small [22,24]. Conversion coefficients for organ equivalent dose ($CC_{HT:KAP}$) were calculated using the same methodology i.e. a single H_T/KAP for each age group.

2.5. Statistical analysis

Linear regression was performed between weight/height and age using Excel (Microsoft Corp., Redmond, WA). This was done to confirm the plausibility of using age as a surrogate for patient size. Adult-size patients in the 15-year age group (i.e. exceeding nominal values of height and/or weight for the adult PCXMC phantom) were excluded from the regression as they would be better mimicked by using an adult phantom in PCXMC. Linear regression was also used to evaluate the correlation between E (and H_T) and KAP. This was performed to evaluate the utility of the conversion coefficient concept: weak correlations indicate little benefit over simply calculating mean doses (E or H_T) for patient groups. Again, adult-size patients were excluded.

The 10th and 90th percentiles for the individual conversion coefficients ($CC_{E:KAP}$ and $CC_{HT:KAP}$) were estimated in MATLAB (MathWorks, Natwick, MA) using the *prctile* function [25]. The percentiles indicate the breadth of the statistical distributions for individuals. Average conversion coefficients were determined as the means of those for all the individual patients in an age group. Confidence Intervals (CIs) were estimated for the coefficients to indicate the uncertainty on the mean values due to finite patient cohorts. The bootstrap sampling technique was used to determine CIs due to evidence of non-normality in the data. The bootstrap calculations were performed in MATLAB using the *bootci* function [25] (BCA method and 10,000 samples).

Non-linear regressions of conversion coefficients (CC) against age were also performed in MATLAB [26] by pooling the patient data without age-grouping. The fitting model was:

$$CC = aexp(-bY) - cY + d \quad (1)$$

where Y is patient age. This provides an alternative estimate of conversion coefficient to those presented for means of age-groupings. Non-linear regression has the benefit of being more robust for small patient cohorts [27] while suffering the disadvantage of assuming accuracy for the fitting function.

All the above statistics were derived from doses calculated using the comprehensive RDSR method. A paired *t*-test was used to evaluate statistical significance in the differences between calculated conversion coefficients for the RDSR and SAM methods. MATLAB's *ttest* function [25] was used to provide the p-values. In addition to E, the H_T for the following organs were tested: active bone marrow, breast, heart, liver, lung, oesophagus and stomach. Since the tests were applied to the pooled set of all patients, the sample size (n = 202) was large enough to ensure the applicability of the tests (the Central Limit Theorem removes issues with non-normality) [28]. A significance level of $\alpha = 0.05$ was assumed.

3. Results

3.1. Equivalent organ dose and effective dose

The distribution of weight and height for the 202 paediatric patients were extracted from HIS and are shown in Fig. 1, together with the standard weight and height of the phantoms used in PCXMC. Three patients in Fig. 1 are highlighted with the symbol (o); the weight and/or height of these patients exceeded nominal paediatric values [19]. Linear regression yielded high correlations between age and weight, and age and height ($R^2 = 0.91$ and 0.92, respectively)

Two important parameters, which are often approximated and fixed at nominal values when estimating doses in the clinic, are the focus-to-skin-distance (FSD) and the collimated beam size. The values for these parameters were extracted from RDSR for the patient cohort and are presented in Table 2 for different age groups and planes (frontal and lateral). Table 2 also shows additional exposure and beam geometry settings extracted from RDSR and used for the dose estimations in PCXMC. Note that the difference in tube potential between fluoroscopy and fluorography is < 4 kV, according to the annual quality assurance measurements performed in the clinic, and is therefore not presented in the table.

The KAP, E and H_T from the entire procedure using the information from RDSR including HIS (Table 1; RDSR method) are reported in

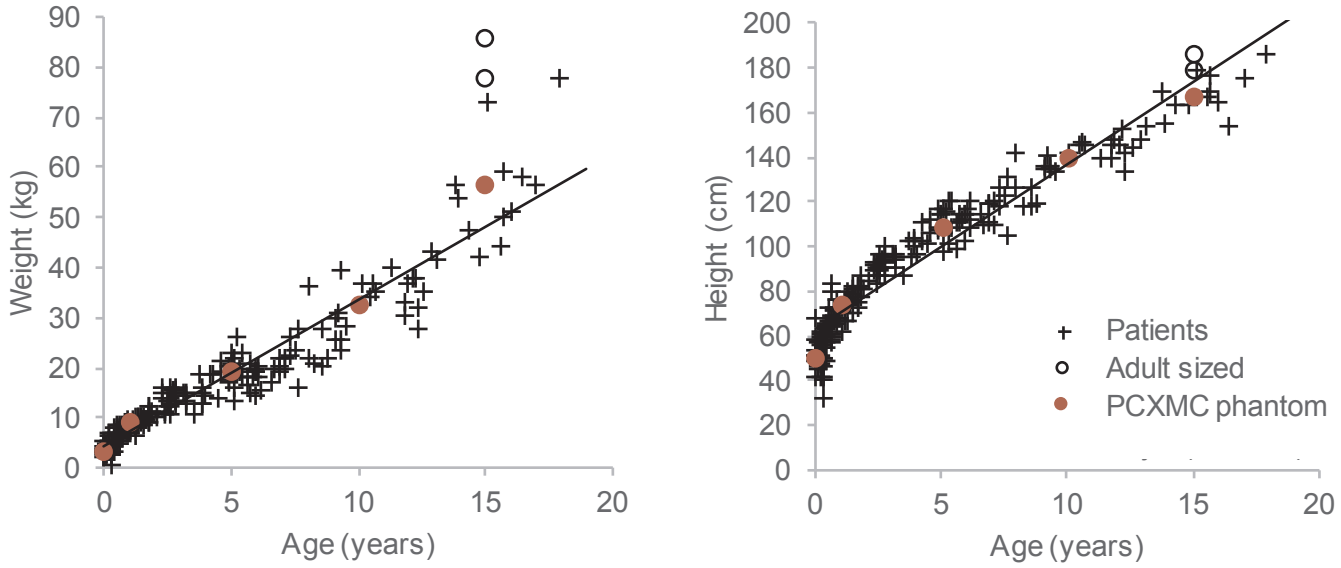

Fig. 1. Distribution of weight and height versus age in the cohort of the 202 patients, together with weight and height data for the phantoms used in PCXMC. The three adult-sized patients are highlights with the symbol (o). The linear equation fitted between weight (X) and age (Y) is: $X = 2.9\,Y + 4.1$ ($R^2 = 0.91$) and between height (Z) and age is: $Z = 7.3\,Y + 64$ ($R^2 = 0.92$).

Table 3. The contribution from the fluoroscopy part of the procedures provided 85 ± 10% (mean ± 1SD) of the total KAP. The organs receiving the highest dose were the lungs in 51% of the patients, the heart in 27% of the patients and the breasts in 21% of the patients, while it was verified (from DICOM images) that the critical organs receiving the lowest doses were outside the radiation beam. The thyroid received < 10% of the equivalent dose to the lungs. Colon, ovaries and bladder received < 4% of the equivalent dose to the lungs. Table 3 also presents the E and H_T (from the entire procedure), estimated with information from SAM (Table 1; SAM).

3.2. Dose conversion coefficient

The conversion coefficients, $CC_{E:KAP}$ and $CC_{HT:KAP}$, calculated with RDSR method, are shown in Table 4 along with their CIs. The conversion coefficients decrease with increasing age.

The relationship between E and KAP shows a good linear correlation for all age groups (R^2 between 0.75 and 0.93). The linear correlations between H_T and KAP for the different organs were: active bone marrow, $R^2 = 0.90–0.99$; breasts, $R^2 = 0.45–0.79$; heart, $R^2 = 0.55–0.96$; liver, $R^2 = 0.55–0.86$; lungs, $R^2 = 0.77–0.97$; oesophagus, $R^2 = 0.78–0.99$; stomach, $R^2 = 0.70–0.96$.

The paired *t*-test for $CC_{E:KAP}$ and $CC_{HT:KAP}$ indicated no statistically significant difference between RDSR and SAM methods for E and active bone marrow, breast, heart, liver and lung dose ($p = 0.074–0.80$). Significance was found, however, for oesophagus ($p = 8.7{\cdot}10^{-5}$) and stomach ($p = 0.021$).

Boxplots for patient $CC_{E:KAP}$ and the $CC_{HT:KAP}$ for heart and for the organs contributing the most to the effective dose (breasts and lungs) are illustrated in Figs. 2 and 3, respectively, for both calculation methods (RDSR and SAM). The plots typically show a wider spread for the conversion coefficients calculated with input values from RDSR,

Table 2
Exposure and beam geometry settings (mean ± 1standard deviation) for 202 patients, extracted from radiation dose structured reports (RDSR).

Age group (years)	Plane	KAP ($Gycm^2$)	Tube potential[1] (kV)	FSD (cm)	Projection angle[2] (deg)	Oblique angle[3] (deg)	Collimated beam size, width (cm)	Collimated beam size, height (cm)
0								
	Frontal	0.36 ± 0.44	67 ± 1.4	69 ± 1.1	87 ± 11	−3.3 ± 5.2	8.6 ± 1.1	8.4 ± 1.2
	Lateral	0.28 ± 0.29	72 ± 2.9	71 ± 0.9	180 ± 1.1	0.43 ± 1.4	6.9 ± 0.84	7.2 ± 1.0
1								
	Frontal	0.50 ± 0.58	69 ± 2.1	67 ± 1.3	84 ± 11	−2.3 ± 3.5	9.4 ± 1.7	9.2 ± 1.5
	Lateral	0.41 ± 0.45	74 ± 3.2	70 ± 0.9	180 ± 1.1	0.77 ± 1.7	7.5 ± 1.1	8.0 ± 1.2
5								
	Frontal	1.3 ± 1.7	70 ± 2.1	66 ± 1.0	85 ± 10	−1.9 ± 5.2	11 ± 1.7	11 ± 1.6
	Lateral	0.45 ± 0.60	76 ± 3.8	67 ± 1.2	180 ± 2.3	0.43 ± 1.9	9.2 ± 1.4	9.5 ± 1.4
10								
	Frontal	2.5 ± 4.5	72 ± 3.0	65 ± 1.2	89 ± 14	−0.84 ± 3.4	11 ± 1.5	11 ± 1.3
	Lateral	1.1 ± 2.6	79 ± 6.5	66 ± 2.6	169 ± 46	0.12 ± 0.82	9.5 ± 1.4	9.5 ± 1.5
15								
	Frontal	9.9 ± 9.5	74 ± 4.9	63 ± 1.3	89 ± 10	−0.65 ± 6.4	10 ± 1.0	10 ± 1.0
	Lateral	8.1 ± 9.9	94 ± 10	62 ± 1.9	174 ± 8.4	0.67 ± 3.2	9.3 ± 0.8	9.5 ± 0.7

KAP, kerma-area product; FSD, focus-skin distance.
[1] Tube potential from fluorography.
[2] Detector rotation angle from right anterior oblique (RAO) to left anterior oblique (LAO) with origin perpendicular to patient's chest.
[3] Detector rotation angle from caudal (CAU) to cranial (CRA) with origin perpendicular to patient's chest.

Table 3
Kerma-area product (KAP; mean, range), effective dose (E; mean, range) and equivalent organ dose (H_T; mean, range) determined for 202 patients using the RDSR and SAM methodology (defined in Table 1). The different organs considered are active bone marrow (abm), breasts, heart, liver, lungs, oesophagus and stomach.

H_T (mSv)									
Age group (years)	KAP ($Gycm^2$)	E (mSv)	abm	Breasts	Heart	Liver	Lungs	Oesophagus	Stomach
0									
RDSR	0.64 (0.050–2.8)	2.1 (0.21–7.2)	0.82 (0.086–3.6)	5.1 (0.42–19)	5.1(0.52–17)	2.4 (0.21–15)	5.4 (0.50–18)	4.4 (0.50–17)	1.4 (0.16–7.2)
SAM		2.6 (0.18–12)	1.0 (0.082–4.7)	5.6 (0.29–28)	6.6 (0.57–32)	2.8 (0.20–12)	7.4 (0.56–35)	6.1 (0.50–30)	1.5 (0.12–6.5)
1									
RDSR	0.91 (0.10–3.6)	1.7 (0.13–6.9)	0.64 (0.068–2.5)	4.1 (0.24–25)	4.9(0.25–23)	1.8 (0.084–5.7)	5.0 (0.51–18)	3.5 (0.21–14)	0.92 (0.057–2.6)
SAM		1.8 (0.093–8.3)	0.63 (0.055–2.8)	4.8 (0.15–26)	5.0 (0.20–22)	1.7 (0.063–7.1)	5.2 (0.36–22)	4.1 (0.20–17)	0.89 (0.040–5.4)
5									
RDSR	1.8 (0.17–11)	1.9 (0.21–9.7)	0.88 (0.073–5.0)	4.0 (0.27–18)	4.4(0.44–19)	1.9 (0.15–11)	5.7 (0.55–29)	3.8 (0.37–19)	1.1 (0.085–6.4)
SAM		2.0 (0.090–14)	0.74 (0.059–4.9)	5.5 (0.12–45)	5.2 (0.22–37)	1.6 (0.056–11)	5.9 (0.36–41)	4.2 (0.20–29)	0.79 (0.036–5.3)
10									
RDSR	3.6 (0.23–22)	2.6 (0.11–18)	1.4 (0.11–8.0)	6.5 (0.086–70)	7.2(0.43–43)	2.3 (0.10–15)	8.0 (0.41–45)	4.5 (0.33–25)	1.0 (0.049–5.7)
SAM		2.4 (0.065–19)	1.1 (0.056–7.7)	6.8 (0.087–60)	6.0 (0.16–45)	2.2 (0.041–19)	7.2 (0.26–52)	4.10 (0.13–32)	0.74 (0.026–5.8)
15									
RDSR	18 (4.3–79)	6.6 (1.4–15)	5.4 (1.5–18)	8.4 (0.94–19)	22(4.5–60)	7.3 (0.74–16)	24.9 (4.5–65)	14 (4.0–33)	2.2 (0.33–4.7)
SAM		6.9 (0.79–28)	4.5 (1.0–20)	12 (0.40–27)	18 (2.0–81)	8.1 (0.42–39)	26 (3.2–126)	13 (2.1–58)	1.8 (0.26–7.3)

compared to SAM.

Non-linear regression of conversion coefficient against age (ungrouped data) yielded excellent correlations for effective dose ($R^2 = 0.98$) and the critical organs of lung ($R^2 = 0.98$) and breast ($R^2 = 0.97$), but a weaker correlation for the heart ($R^2 = 0.65$). The fit coefficients are presented in Table 5.

4. Discussion

The minimum number of patients recommended for a study of this type is, according to the ICRP 135 [29], 30 patients per age group. Except for the 10-years (27 patients) and 15-years (16 patients) group, this condition was satisfied. We note the difficulty in accumulating sufficient numbers in the older groups and emphasize that confidence intervals were quoted on conversion coefficients. There exists no standard on age groupings, but following the ICRP [30,31] we adopted the groupings of 0, 1, 5, 10, 15 years, which has also been used in other publications, thus facilitating comparisons between these studies.

Another limitation of this study important to acknowledge, are potential errors caused by the phantom models used in PCXMC for the dose calculations. The use of stylized phantoms, as in PCXMC, has been observed in some cases to produce considerable errors [32,33]. However, the errors observed were substantial mainly for abdominal examinations, due to the incorrect representation of the distribution of fatty tissue in a stylized phantom. For cardiac examinations, the same studies indicated a smaller variation in calculated average organ doses (in the order of 0–40%), with a better agreement for younger phantom models. These results are also supported by the findings of Smans et al. [34], who concluded that the phantoms used in PCXMC for prematurely born babies were sufficiently accurate compared with voxelized phantoms for organ dose estimations.

The E values reported in this study are of the same magnitude as

Table 4
Conversion coefficients for effective doses ($CC_{E:KAP}$) and equivalent organ doses ($CC_{HT:KAP}$) estimated with the RDSR method (defined in Table 1) for 202 paediatric patients that have undergone cardiac interventions. The different organs considered are active bone marrow (abm), breast, heart, liver, lung, oesophagus, and stomach. The values are presented as mean with Confidence Interval (CI), median and 10th/90th centile.

	Conversion coefficients for effective dose and equivalent organ dose ($mSv/Gycm^2$)							
Age group (years)	CC_E	CC_{abm}	$CC_{breasts}$	CC_{heart}	CC_{liver}	CC_{lungs}	$CC_{oesophagus}$	$CC_{stomach}$
0								
Mean [CI]	3.6 [3.3, 4.0]	1.4 [1.3, 1.6]	8.9 [7.8, 10]	9.3 [8.3, 10]	3.9 [3.3, 4.7]	9.4 [8.7, 10]	7.7 [7.0, 8.4]	2.3 [1.9, 2.7]
Median	3.4	1.3	8.4	9.5	3.2	9.0	7.2	1.9
10th/90th centile	2.3/5.1	0.87/1.8	4.4/14	5.2/14	1.8/7.2	6.4/14	4.9/11	1.2/4.0
1								
Mean [CI]	2.0 [1.8, 2.2]	0.73 [0.70, 0.77]	4.8 [4.2, 5.6]	5.8 [5.1, 6.5]	2.1 [1.9, 2.4]	5.7 [5.3, 6.1]	4.0 [3.6, 4.4]	1.1 [1.0, 1.2]
Median	1.8	0.70	3.8	6.1	1.9	5.6	3.4	1.0
10th/90th centile	1.2/3.0	0.57/0.95	1.9/8.9	2.4/9.9	1.1/3.2	4.1/7.5	2.3/6.3	0.63/1.6
5								
Mean [CI]	1.1 [1.1, 1.2]	0.49 [0.47, 0.51]	2.6 [2.2, 3.1]	3.0 [2.7, 3.3]	1.1 [1.0, 1.3]	3.4 [3.2, 3.6]	2.3 [2.1, 2.4]	0.60 [0.57, 0.64]
Median	1.1	0.48	2.1	2.7	1.1	3.4	2.3	0.59
10th/90th centile	0.78/1.7	0.39/0.63	1.1/5.4	1.5/5.3	0.57/1.9	2.6/4.4	1.5/3.1	0.42/0.83
10								
Mean [CI]	0.77 [0.68, 0.85]	0.42 [0.39, 0.46]	1.7 [1.4, 2.2]	2.3 [2.0, 2.7]	0.80 [0.67, 1.0]	2.4 [2.2, 2.7]	1.4 [1.3, 1.5]	0.33 [0.28, 0.41]
Median	0.76	0.41	1.5	2.2	0.68	2.4	1.3	0.28
10th/90th centile	0.46/1.0	0.32/0.54	0.40/3.5	1.2/3.7	0.42/1.5	1.7/3.3	1.1/1.8	0.17/0.52
15								
Mean [CI]	0.42 [0.36, 0.47]	0.34 [0.31, 0.38]	0.54 [0.41, 0.68]	1.4 [1.2, 1.6]	0.45 [0.36, 0.56]	1.6 [1.3, 1.8]	0.93 [0.79, 1.0]	0.15 [0.12, 0.18]
Median	0.43	0.33	0.58	1.3	0.46	1.5	0.96	0.17
10th/90th centile	0.29/0.55	0.24/0.44	0.16/0.88	0.89/2.1	0.18/0.70	0.85/2.2	0.62/1.2	0.061/0.22

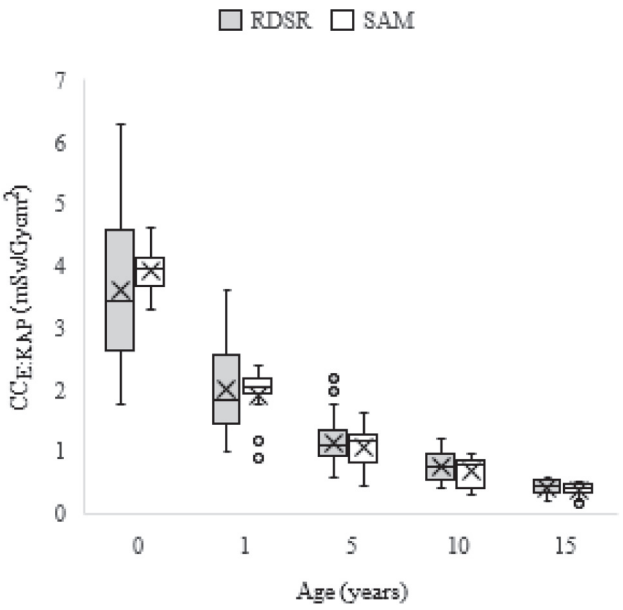

Fig. 2. Conversion coefficient for effective dose ($CC_{E:KAP}$) for the five age groups (0, 1, 5, 10, 15) presented as boxplots, for both the RDSR and simplified SAM calculation methods. The mean (cross), median (horizontal line), interquartile range (box) and range (vertical line) are displayed.

those reported by Harbron et al. [13], Ubeda et al. [14] and Barnaoui et al. [12] and lower than the E reported by Yakoumakis et al. [11] and Song et al. [35]. The higher E from Yakoumakis et al. [11] and Song et al. [35] could be related to a lower total filtration and/or less collimated beam in their study. In addition, the equipment used in the study by Yakoumakis et al. [11] was based on image intensifier technology. Such detectors are known to contribute to higher doses in general. The organs contributing the most to the effective dose were, as expected from beam geometry and tissue weighting factors (w_T), the lungs and breasts (see Table 3). These organs are also identified as critical organs in the paper by Yakoumakis et al. [11], Barnaoui et al. [12], Harbron et al. [13] and Ubede et al. [14], independent to procedure type and age. Comparing these organ doses, while the current study yielded similar dose values to breasts and lungs, the study by Barnaoui et al. [12] and Ubeda et al. [14] reported higher doses to the lungs compared to breasts. This could indicate differences in beam geometry (projection angle and planes) and/or difference in collimated beam size. In the paper by Yakoumakis et al. [11] the situation was reversed, that is a higher dose to the breasts compared to the lungs. This could reflect also, differences in the relative use of the two detector planes during the procedure, compared to our study.

The heart does not contribute substantially to E, yet is indeed a critical organ with respect to circulatory disease. The ICRP 118 [36] has suggested a threshold value of 0.5 Gy for radiation induced circulatory disease and this value has not been exceeded in the patient sample analysed in this work. However, it is worth noting that paediatric patients that undergo multiple procedures could potentially exceed the threshold, and considering that children are more sensitive than adults to radiation induced circulation disease [37], awareness of the risk is advised.

There are few studies reporting H_T from paediatric cardiac interventions. The study by Yakoumakis et al. [11] which included a patient cohort of 53 patients (3 months-11 years) and grouped according to the type of heart disorder (ASD, VSD, PDA), reported the highest H_T to thymus (65–175 mSv), heart (60–145 mSv), breasts (60–140 mSv) and lungs (25–65 mSv). These doses are considerably higher compared to the H_T reported here, and is interpreted to reflect the use of an older type of x-ray system based on image intensifiers technology. Further,

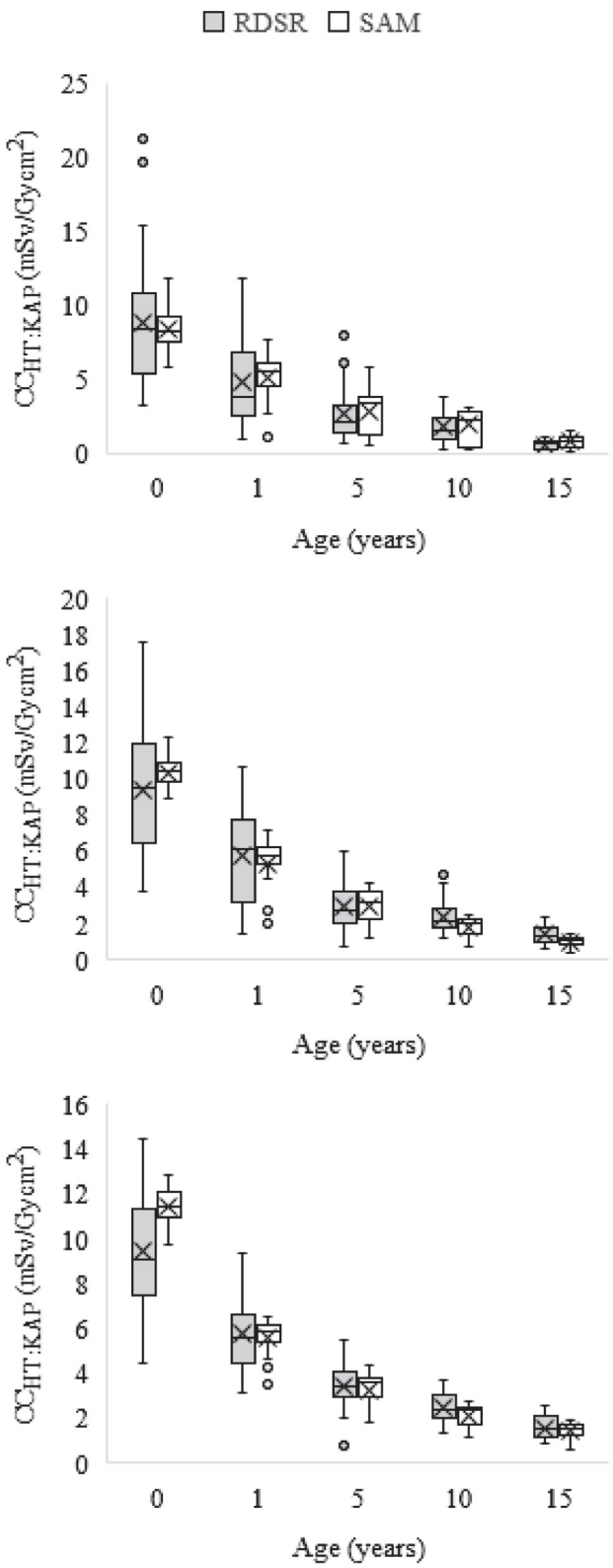

Fig. 3. Conversion coefficients for equivalent organ doses (CC_{HT}:KAP) for the five age groups (0, 1, 5, 10, 15) presented as boxplots, for both the RDSR and simplified SAM calculation methods, for (top) breast, (middle) heart and (bottom) lung. The mean (cross), median (horizontal line), interquartile range (box) and range (vertical line) are displayed.

Table 5
Non-linear fits to conversion coefficients for effective doses ($CC_{E:KAP}$) and equivalent organ doses ($CC_{HT:KAP}$) for breast, heart and lung. The calculations were performed with the RDSR method (defined in Table 1). The non-linear fitting model was: CC = a exp(−b Y) − c Y + d, Y = age. Coefficients of variation (R^2) were 0.98, 0.97, 0.67 and 0.98 for effective dose, breast, heart and lung, respectively.

Conversion coefficient	a (mSv/Gycm^2)	b (1/y)	c (mSv/Gycm^2/y)	d (mSv/Gycm^2)
CC_E	3.0	1.5	0.061	1.4
$CC_{breasts}$	8.1	1.3	0.14	2.7
CC_{heart}	7.4	−0.89	0.096	3.0
CC_{lungs}	6.4	−1.2	0.16	4.0

the paper by Harbron [13] included a large volume of patients and the most recent collections (3000 patients, 2008–2013, data from hospitals referred to as hospital 2 and 3 in the paper) can be compared to the present study. The reported H_T from hospital 3 were of the same magnitude as in this work, while higher H_T were reported from hospital 2 (lung and heart, 23 mSv; breast, 19 mSv). Another study [12] estimated H_T with phantom measurements and showed highest dose in lungs (2–61 mSv), esophagus (4–54 mSv) and breasts (1–33 mSv). A recently published paper [14] including 1500 patient reported organ doses slightly lower than those reported in this work; they reported that the highest organ dose was the lung (5 mSv).

The picture is therefore complicated with regard to patient doses, and it is likely that differences in clinical practice, model of angiographic equipment and machine settings play a substantial role in explaining discrepancies between studies. The KAP-values presented here are similar to those reported by Barnaoui et al. [12], Harbron et al (2008–2013) [13] and Ubeda et al. [14] and significantly lower than those reported by Yakoumakis et al. [11], Song et al. [35] and Kottou et al. [38]. It should be noted that fluoroscopy time is a parameter reported in many studies. However, since it is known to be badly correlated with patient dose, it has not been included in the present study.

Conversion coefficients provide a convenient method of estimating dose. The approach also has the advantage of factoring out the component of variability in doses due to varying KAP values. The $CC_{E:KAP}$ presented here using RDSR data are consistent with those calculated using older equipment that did not support the extraction of procedure-specific data from RDSR [11,22,24]. Furthermore, conversion coefficients for organ doses were established for different age groups (Table 4) and are intended to be used for estimation of H_T on a routine basis for clinics that do not have the facility for extraction of examination settings and/or using a Monte Carlo system like PCXMC.

Statistical significance was only identified between dose conversion coefficients calculated using the RDSR and SAM methods for the oesophagus and stomach. Since the former organ has a relatively low tissue weighting factor and the latter organ typically received low doses compared to the lung and breast, the RDSR and SAM approaches can effectively be considered equivalent for calculations of mean doses for populations. The agreement is not unexpected, if the fixed input parameters selected for SAM (e.g. collimated beam size and FSD) are close to the average values for the RDSR data (see Table 2).

A potential use of the conversion coefficients presented in this study is as input to epidemiological studies of dose-response involving large paediatric cohorts. We observed that organ dose was not always strongly correlated to KAP, implying that the utility of the conversion coefficient concept becomes weak in some cases. For example, the H_T to breast was not strongly correlated to KAP even with subdivision into age groups. We believe this reflects the varying proportion of the breast tissue being irradiated [39]. None the less the use of conversion coefficients to calculate average population organ doses, based on the patient ages and the KAP-values from the examinations, could be acceptable for retrospective studies.

For individual patient cases, however, conversion coefficients are of limited value and a more rigorous calculation method is preferred such as the full RDSR approach. Although no important statistical significances were identified between mean conversion coefficients, the RDSR method typically displays a greater spread in individual values compared to the SAM approach (see boxplots in Figs. 2 and 3). This is also reflected in the statistics presented in Table 4, where the 10th, 50th and 90th percentiles of the conversion coefficients show a wide separation (as derived from the calculations using RDSR data and PCXMC). These uncertainties can be assumed to be representative of realistic clinical patient-to-patient variability, unlike those based on fixed values of parameters such as collimated beam size. Despite these uncertainties in a particular patient's conversion coefficients, the concept can still be of some use for individual cases. A coverage interval on a dose estimate can be constructed, based on the quoted percentiles (10%, 50% and 90%). For example, a patient can be estimated as having a 90% chance of having an organ dose less than the 90th percentile of a conversion coefficient multiplied by the appropriate KAP value.

Finally, we note that this study reports typical patient dose levels from paediatric cardiac interventions performed on state-of-the-art radiological equipment incorporating modern dose reduction technology [40–42] and high total filtration.

5. Conclusion

Effective dose (E), equivalent organ doses (H_T) and associated conversion coefficients were estimated for paediatric cardiac interventions, using procedure-specific data from radiation dose structured reports (RDSR). These were compared with estimates based on data from patient radiation dose sheets where assumptions were made for the missing information; a more approximate and simplified methodology. The results presented for population-averaged conversion coefficients did not display significant differences (for E and H_T in critical organs receiving high doses).

Notably, to our knowledge this work constitutes the first publication of age-based organ dose conversion coefficients ($CC_{HT:KAP}$) for paediatric patients in interventional cardiac radiology. This quantity allows the estimation of H_T in retrospective epidemiological studies. It can also be used to assist in assessment of the effects on organ dose when new or modified irradiation techniques are introduced. However, Monte Carlo calculations using RDSR information are recommended when individual dose estimates are desired.

Acknowledgements

The authors are grateful to Robert Vorbau for help with parsing radiation dose structured reports and Eva Kvanta for providing necessary information on procedures within paediatric interventional cardiac radiology.

Declaration of Interest

None.

Funding

This research received no specific grant from any funding agency in the public, commercial, or not-for-profit sectors.

References

[1] UNSCEAR. Effects of ionizing radiation. Report to the General Assembly of the United Nations. New York, NY; 2006.
[2] ICRP 85 International Commission on Radiological Protection. Avoidance of Radiation Injuries from Medical Interventional Procedures. Publication 85. Ann.

ICRP 30 (2), 2000.
[3] ICRP 60 International Commission on Radiological Protection. Recommendations of the International Commission on Radiological Protection. Publication 60. Ann. ICRP 21 (1-3), 1991.
[4] Darby SC. Epidemiological evaluation of radiation risk using population exposed at high doses. Health Phys 1986;51:269–81.
[5] Bacher K, Bogaert E, Lapere R, De Wolf D, Thierens H. Patient-specific dose and radiation risk estimation in pediatric cardiac catheterization. Circulation 2005;111:83–9.
[6] Li LB, Kai M, Kusama T. Radiation exposure to patients during paediatric cardiac catheterisation. Radiat Prot Dosimetry 2001;94:323–7.
[7] Holzer R, Hijazi ZM. Interventional approach to congenital heart disease. Curr Opin Cardiol 2004;19:84–90.
[8] Patel HT, Hijazi ZM. Pediatric catheter interventions: a year in review 2004–2005. Curr Opin Pediatr 2005;17(5):568–73.
[9] Hill KD, Frush DP, Han BK, Abbott BG, Armstrong AK, DeKemp RA, et al. Radiation safety in children with congenital and acquired heart disease: a scientific position statement on multimodality dose optimization from the image gently alliance. JACC Cardiovasc Imag 2017;10(7):797–818.
[10] Committee to Assess Health Risks from Exposure to Low Levels of Ionizing Radiation; Nuclear and Radiation Studies Board, Division on Earth and Life Studies, National Research Council of the National Academies. Health risks from exposure to low levels of ionizing radiation: BEIR VII Phase 2. Washington, DC:The National Academies Press, 2006.
[11] Yakoumakis E, Kostopoulou H, Makri T, Dimitriadis A, Georgiou E, Tsalafoutas I. Estimation of radiation dose and risk to children undergoing cardiac catheterization for the treatment of a congenital heart disease using Monte Carlo simulations. Pediatr Radiol 2013;43:339–46.
[12] Barnaoui S, Rehel JL, Baysson H, Boudjemline Y, Girodon B, Bernier MO, et al. Local reference levels and organ doses from pediatric cardiac interventional procedures. Pediatr Cardiol 2014;35:1037–45.
[13] Harbron RW, Pearce MS, Salotti JA, McHugh K, McLaren C, Abernethy L, et al. Radiation doses from fluoroscopically guided cardiac catheterization procedures in children and young adults in the United Kingdom: A multicentre study. Br J Radiol 2015;88:20140852.
[14] Ubeda C, Miranda P, Vano E, Nocetti D, Manterola C. Organ and effective doses from paediatric interventional cardiology procedures in Chile. Phys Med. 2017;40:95–103.
[15] DICOM 2005 Supplement 94: Diagnostic x-ray radiation dose reporting (Dose SR) National Electrical Manufacturers Association (NEMA) Rosslyn, Virginia; 2005.
[16] Omar A, Bujila R, Fransson A, Andreo P, Poludniowski G. A framework for organ dose estimation in x-ray angiography and interventional radiology based on dose-related data in DICOM structured reports. Phys Med Biol 2016;61:3063–83.
[17] Toroi P, Komppa T, Kosunen A. A tandem calibration method for kerma-area product meters. Phys Med Biol. 2008;53(18):4941–58.
[18] Gislason AJ, Hoornaert B, Davies AG, Cowen AR. Allura Xper Cardiac System Implementation of Automatic Dose Rate Control (ADRC). Philips Healthcare Publication; 2011.
[19] Tapiovaara M, Lakkisto M, Servomaa APCXMC. A Monte Carlo Program for Calculating Patient Doses in Medical x-ray Examinations. (2nd Ed.) Helsinki: Finnish Centre for Radiation Nuclear Safety; 2008. Report STUK-A231.
[20] ICRP 103 International Commission on Radiological Protection. The 2007 recommendations of the international commission on radiological protection, ICRP publication 103. Ann. ICRP 37(2-4), 2007.
[21] Cristy M and Eckerman K F 1987 Specific absorbed fractions of energy at various ages from internal photon sources. I. Methods. Report/TM-8381/V1 Oak Ridge National Laboratory Oak Ridge, TN.
[22] Karambatsakidou A, Sahlgren B, Hansson B, Lidegran M, Fransson A. Effective dose conversion factor in paediatric interventional cardiology. Br J Radiol 2009;82:748–55.
[23] Brambilla M, Cannillo B, Matheoud R, Compagnone G, Rognoni A, Bongo AS, et al. Conversion factors of effective and equivalent organ doses with the air kerma area product in patients undergoing coronary angiography and percutaneous coronary interventions. Phys Med. 2017;42:189–96.
[24] Axelsson B, Khalil C, Lidegran M, Schuwert P, Mortensson W. Estimating the effective dose to children undergoing heart investigations-a phantom study. Br J Radiol 1999;72:378–83.
[25] MATLAB and Statistics and Machine Learning Toolbox Release 2017b, The MathWorks, Inc., Natick, Massachusetts, United States.
[26] MATLAB and Curve Fitting Toolbox Release 2017b, The MathWorks, Inc., Natick, Massachusetts, United States.
[27] H. Järvinen, R. Seuri,M. Kortesniemi, A. Lajunen, E. Hallinen, P. Savikurki-Heikkilä, P. Laarne, M. Perhomaa and E. Tyrvainen. Indication-based national diagnostic reference levels for paediatric CT: A new approach with proposed values. Radiat Prot Dosimetry 2015;165:No. 1–4:86–90.
[28] Norman G. Likert scales, levels of measurement and the “laws” of statistics. Adv Health Sci Educ Theory Pract. 2010;15(5):625–32.
[29] ICRP, 2017. Diagnostic reference levels in medical imaging. ICRP Publication 135. Ann. ICRP 46(1).
[30] ICRP, 2007b. Managing patient dose in multi-detector computed tomography (MDCT).
[31] ICRP, 2013b. Radiological protection in paediatric diagnostic and interventional radiology.
[32] Johnson PB, Geyer A, Borrego D, Ficarrotta K, Johnson K, Bolch WE. The impact of anthropometric patient-phantom matching on organ dose: a hybrid phantom study for fluoroscopy guided interventions Med. Phys. 38 1008–17Martin CJ. Effective dose: how should it be applied to medical exposures? Br J Radiol. 2011;80(956):639–47.
[33] Borrego D, Lowe EM, Kitahara CM, Lee C. Assessment of PCXMC for patients with different body size in chest and abdominal x ray examinations: a Monte Carlo simulation study. Phys Med Biol 2018;63(6):065015.
[34] Smans K, Tapiovaara M, Cannie M, Struelens L, Vanhavere F, Smet M, et al. Calculation of organ doses in x-ray examinations of premature babies. Med Phys. 2008;35(2):556–68.
[35] Song S, Liu C, Zhang M. Radiation dose and mortality risk to children undergoing therapeutic interventional cardiology. Acta Radiol 2015;56:867–72.
[36] ICRP 118 International Commission on Radiological Protection. Statement on tissue reactions, and early and late effects of radiation in normal tissues and organs – threshold doses for tissue reactions in a radiation protection context. ICRP publication 118. Ann. ICRP 41(1/2), 2012.
[37] Tukenova M, Guibout C, Oberlin O, Doyon F, Mousannif A, Haddy N, et al. Role of cancer treatment in long-term overall and cardiovascular mortality after childhood cancer. J. Clin. Oncol 2010;28:1308–15.
[38] Kottou S, Kollaros N, Plemmenos C, Mastorakou I, Apostolopoulou SC, Tsapaki V. Towards the definition of Institutional diagnostic reference levels in paediatric interventional cardiology procedures in Greece. Phys Med. 2018;46:52–8.
[39] Rassow J, Schmaltz AA, Hentrich F, Streffer C. Effective doses to patients from pediatric cardiac catheterization. Br J Radiol 2000;73:172–83.
[40] Söderman M, Mauti M, Boon S, Omar A, Marteinsdó ttir M, Andersson T, Holmin S, Hoornaert B. Radiation dose in neuroangiography using image noise reduction technology: a population study based on 614 patients. Neuroradiology 2013;55:1365–72.
[41] Nakamura S, Kobayashi T, Funatsu A, Okada T, Mauti M, Waizumi Y, et al. Patient radiation dose reduction using an X-ray imaging noise reduction technology for cardiac angiography and intervention. Heart Vessels 2015. https://doi.org/10.1007/s00380-015-0667-z.
[42] Haas NA, Happel CM, Mauti M, Sahyoun C, Tebart LZ, Kececioglu D, et al. Substantial radiation reduction in pediatric and adult congenital heart disease interventions with a novel x-ray imaging technology. Int. J. Cardiol. Heart Vasc. 2015;6:101–9.